SAR-ISAR Blending Using Compressed Sensing Methods

Larsson, Christer; Jersblad, Johan

Published in:
AMTA Proceedings

2015

SAR-ISAR Blending Using Compressed Sensing Methods

Christer Larsson
Saab Dynamics
SE-581 88 Linköping, Sweden

Lund University
P.O. Box 118, SE-221 00 Lund, Sweden

Johan Jersblad
Saab Barracuda
SE-594 32 Gamleby, Sweden

***Abstract*—Inverse Synthetic Aperture Radar (ISAR) target images are extracted using compressed sensing methods. The extracted images are edited and merged into measured Synthetic Aperture Radar (SAR) images. A noise free image of the target is extracted from the Radar Cross Section (RCS) measurement by using the Basis Pursuit Denoise (BPDN) method and then solving for a model consisting of point scatterers. The target signature point scatterers are then merged into a point scatterer representation of the SAR background scene. This method means that SAR images acquired in expensive airborne field trials can be used efficiently to evaluate different targets and camouflage measured separately in a ground based setup. The method is demonstrated with turntable measurements of a full scale target, with and without camouflage, signature extraction and blending into a SAR background. We find that the method provides an efficient way of evaluating measured target signatures in SAR backgrounds.**

I. Introduction

Different methods can be used in order to protect vehicles and structures from being detected by air or satellite based Synthetic Aperture Radar (SAR) systems. One method is to use camouflage *e.g.*, in the forms of nets or mobile camouflage systems. The efficiency of these camouflage systems then have to be evaluated with the target placed in different backgrounds.

The evaluation method that first comes to mind is to use airborne SAR field trials. Ideally, each target should then be measured for many orientations as well as illumination angles which would result in a large number of measurement cases. Data from one such comprehensive measurement campaign, Moving and Stationary Target Acquisition and Recognition (MSTAR), that was collected to provide data for research in automatic target recognition is available for download [1].

Figure 1 is an example of a SAR image of a T-72 tank taken from the MSTAR data set. Typical features for SAR images are visible in this image, such as the target itself, ground clutter and the target shadow. Note also that contributions from system noise are visible in the otherwise dark blue target shadow.

The main disadvantages with using airborne SAR-systems are that such measurements are complicated and expensive. Furthermore, in the application that we are addressing here, one would like to compare the effects of different camouflage systems on the same target for many different angles. Using an airborne SAR-system for all combinations of configurations, camouflage systems and angles would be very time consuming. Reproducibility is another aspect that has to be taken into account. It is hard to measure repeatedly in a consistent way at the same angles.

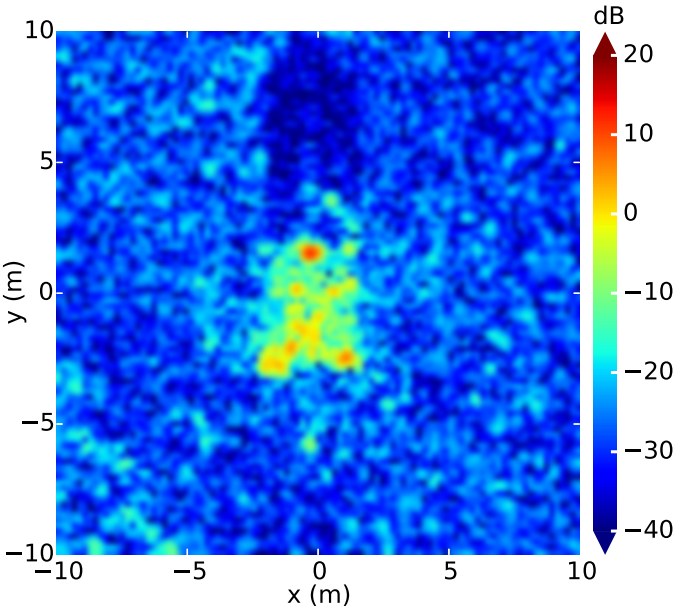

Fig. 1. X-band SAR front aspect image of a T-72 tank from the MSTAR data set [1].

A more cost effective solution is to use ground based ISAR measurements of the desired targets with or without camouflage systems and then blend these ISAR images into the SAR scene. This means that the SAR-data can be reused for many different target measurements. The merging of the data should then be performed as a part of the imaging process to get realistic composite images that are free from editing artifacts. An example of a method where that is done is

described in [2] where the merging of the ISAR and SAR data is done as a part of doing the down range processing step.

Compressed sensing methods are used in this study. The compressed sensing field, sometimes called compressive sensing, was pioneered about 10 years ago by [3], [4]. It is basically a method to solve an underdetermined system of equations iteratively by assuming a sparse solution. There are many potential application areas for compressed sensing including radar imaging [5].

This study presents a method where the inverse scattering problem is solved for a model consisting of isotropic point scatters using a compressed sensing method. The point scatters are then blended with an edited point scatterer representation of the background.

II. Theory

This study presents an approach where the RCS turntable measurement data from the target is used to solve an inverse problem consisting of isotropic point scatterers in the image domain. The system of equations describing the model can be written

$$\boldsymbol{A}\boldsymbol{z} = \boldsymbol{b}, \tag{1}$$

where $\boldsymbol{A}$ is the forward operator, $\boldsymbol{z} = \boldsymbol{z}(x, y)$ contains the isotropic point scatterers, and $\boldsymbol{b} = \boldsymbol{b}(f, \varphi)$ is the measured RCS. This is shown graphically in (2).

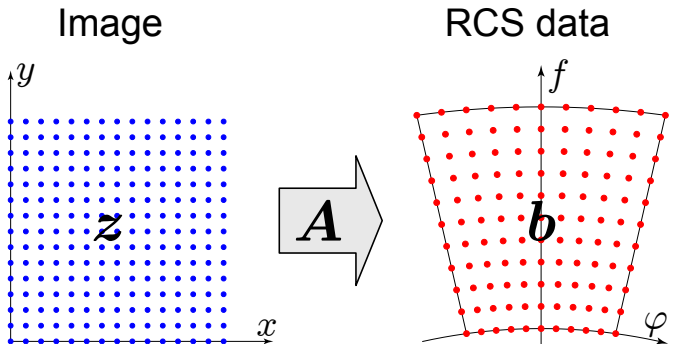

Fig. 2. The sparse matrix containing the isotropic point scatters, $\boldsymbol{z}$, the forward operator $\boldsymbol{A}$ and the resulting RCS stored in matrix $\boldsymbol{b}$.

The model as defined by the forward operator $\boldsymbol{A}$ is constructed so that the point scatters are fixed to the turntable, isotropic and have constant amplitude for all frequencies. The solution to the system of equations is naturally sparse, *i.e.*, few scatterers are required to describe the measured RCS meaning that most elements in $\boldsymbol{z}(x, y)$ are zero. The compressed sensing method Basis Pursuit Denoise (BPDN) implemented in SPGL1 is used to extract the point scatterer locations and amplitude [6], [7]. The BPDN problem is formulated as

$$\text{Minimize } ||\boldsymbol{z}||_1 \text{ subject to } ||\boldsymbol{A}\boldsymbol{z} - \boldsymbol{b}||_2 \leq \sigma, \tag{2}$$

where the indices 1 and 2 denote the ℓ_1 and ℓ_2 norms, respectively. σ is an estimate of the noise. Using BPDN described by (2) will promote sparsity in the solution for $\boldsymbol{z}$ [6], [7]. The point scatterers represented by the matrix $\boldsymbol{z}$ then results in noise free RCS if operated on by the forward operator $\boldsymbol{A}$. This part of the method is similar to previous work in [8] and [9]. A near field formulation for $\boldsymbol{A}$ is used in our implementation.

Equation (1) can also be solved directly using back projection which is a standard method for ISAR imaging [10], [11]. $\boldsymbol{z}(x, y)$ is then given by

$$\boldsymbol{z}(x, y) = \sum_{\mathrm{m}=1}^{\mathrm{M}} \sum_{\mathrm{n}=1}^{\mathrm{N}} K_{\mathrm{m}} \boldsymbol{b}(f_{\mathrm{n}}, \mathrm{m}) \mathrm{e}^{(-\mathrm{i}2k_{\mathrm{n}}(r_{\mathrm{m}}(x,y) - r_{\mathrm{m}0}))} f_{\mathrm{n}} \tag{3}$$

for M antenna positions and N frequencies. $r_{\mathrm{m}}(x, y)$ is the distance from the antenna to (x, y) and $r_{\mathrm{m}0}$ is the distance from the antenna to the origin. K_{m} is a normalization constant given by

$$K_{\mathrm{m}} = \left(\frac{1}{\mathrm{MN}}\right) \left(\frac{r_{\mathrm{m}}(x, y)}{r_{\mathrm{m}0} f_{\mathrm{c}}}\right)^2 \tag{4}$$

where f_{c} is the center frequency.

Both BPDN and back projection are used in this study. BPDN is used to generate the point scatterer representation of the target and back projection is used to generate the SAR and ISAR images.

III. Method

The RCS measurement data from the target is used to solve an inverse problem consisting of isotropic point scatterers as described previously. This part of the method is similar to previous work in [8] and [9]. The SAR background is then generated synthetically from point scatterers extracted from a background SAR measurement in this study. The background is edited to approximate the effect of a shadow and attenuation through camouflage. The target and background point scatterers are merged and the forward operator $\boldsymbol{A}$ to obtain RCS data that is used to make a blended SAR image through back projection.

The method can be summarized in the following steps:

1) Perform a target measurement to aquire the complex RCS data, $\boldsymbol{b}(f_{\mathrm{n}}, \mathrm{m})$.
2) Use the BPDN method to determine the point scatterer representation $\boldsymbol{z}(x, y)$ for the target.
3) Edit $\boldsymbol{z}(x, y)$ to only contain the target scatterers.
4) Generate a point scatterer background.
5) Overlay the target shadow on the background point scatterers. Remove the point scatters that are in the shadow.
6) If there is camouflage then overlay the camouflage shadow on the background point scatterers. Attenuate the point scatters that are in the shadow.
7) Combine the edited point scatterer background with the target point scatters. Use the forward operator, $\boldsymbol{A}$, to generate the corresponding RCS.
8) Add noise to the RCS to simulate the performance of the SAR system.
9) Use the RCS to generate a blended SAR-ISAR image with back projection.

The effects of multiple scattering from target-ground interactions are not taken into account in the method presented here.

IV. Results and Discussion

Measured X-band data from a full scale target are used to demonstrate the method. Measured data from a STANDCAM (Standard Decoy for Camouflage Materials) is used for this purpose, see Fig. 3. This non-classified target is developed by WTD 52, Oberjettenberg, Germany and is made from metallized glass-fiber reinforced plastic. The right side is wheeled and the left side is tracked in order to simplify comparisons between wheeled and tracked alternatives of a vehicle.

The generic camouflage net is based on a warp-knitted polyester coated with an electrically conductive coating. The surface resistance of the material is typically $200\,\Omega/\square$. The interaction between the material and the radar wave is a combination of transmission, reflection and absorption. The internal structure, *i.e.*, distance between the yarns and roughness, of the coated fabric is much smaller than the wavelength of the incoming waves. More information about the camouflage and analysis of its effectiveness can be found in [12].

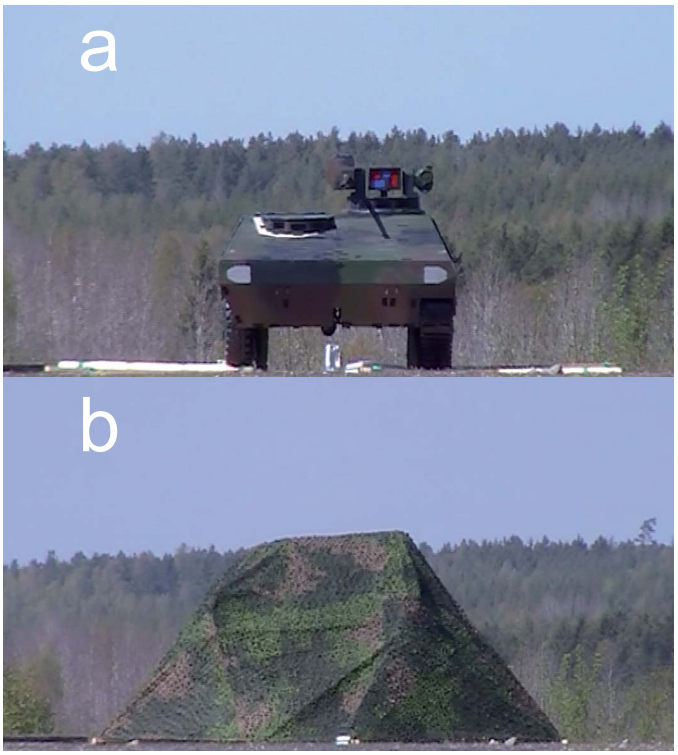

Fig. 3. The STANDCAM test target, without (a) and with camouflage (b).

The measurements were performed at a center frequency of 10 GHz. Data with a bandwidth of 0.5 GHz with VV polarization and 2.8° angular width was used for the processing for the images presented in this paper. This gives a resolution of about 0.3 m in both down and cross range. A Hanning window was used for all data processed with back projection. The distance between the measurement radar and the target was $r_0 = 163$ m. The measurements were performed at the Swedish Defence Research Agency (FOI) outdoor measurement range.

Fig. 4 shows an ISAR image of the target without camouflage and Fig. 5 shows an ISAR image of the target with camouflage. Both images are processed using back projection. The images show that the camouflage attenuates the signature.

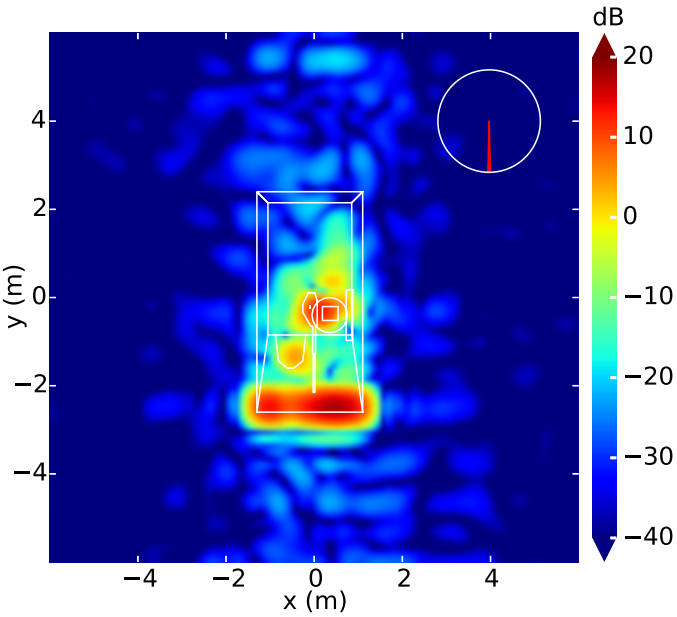

Fig. 4. Back projection ISAR image of the target without camouflage. The filled circle sector shows the part of the angle interval that is used for the image.

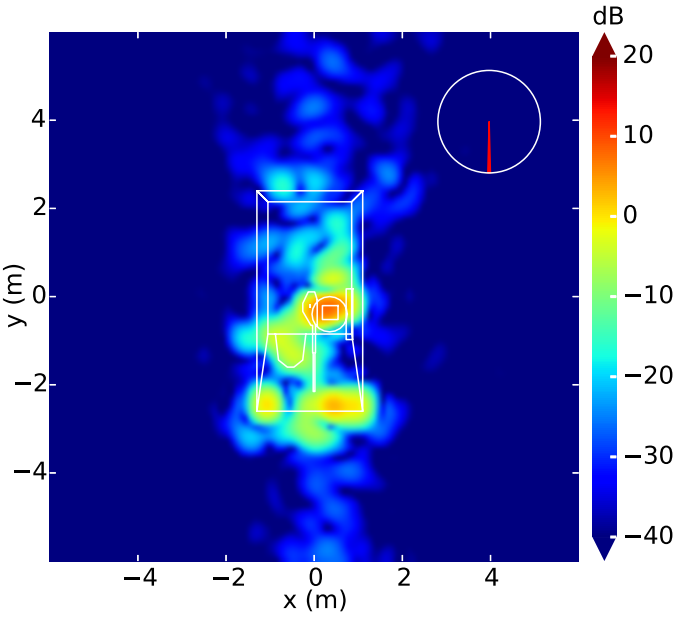

Fig. 5. Back projection ISAR image of the target with camouflage. The filled circle sector shows the part of the angle interval that is used for the image.

The BPDN method is then used to solve the inverse problem defined by (1). This results in a sparse solution with scatterers

and their amplitudes. This is shown in the left frames of Figs. 6 and 7 for the uncamouflaged and camouflaged targets, respectively. The right frames show the corresponding back projection ISAR images processed from the RCS generated by the forward operator, $\boldsymbol{A}$, operating on the matrix containing the point scatterer amplitudes.

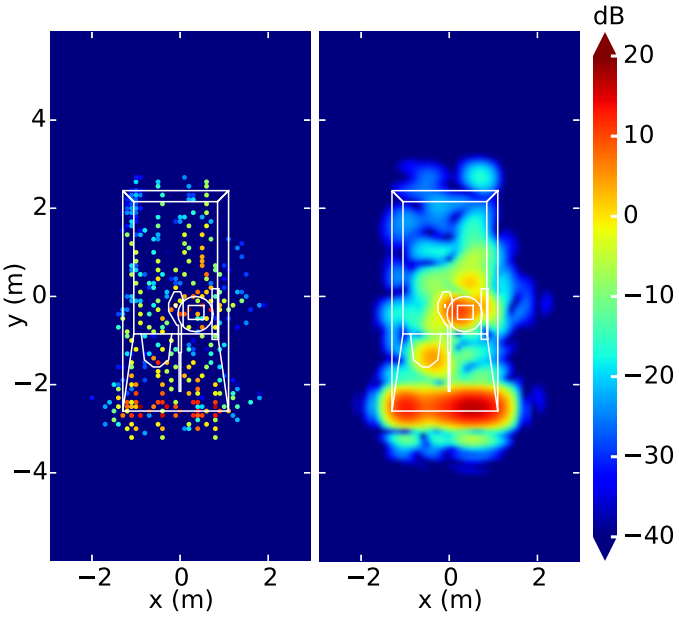

Fig. 6. Isotropic point reflector representation (left) and the corresponding back projection ISAR image (right) for the target.

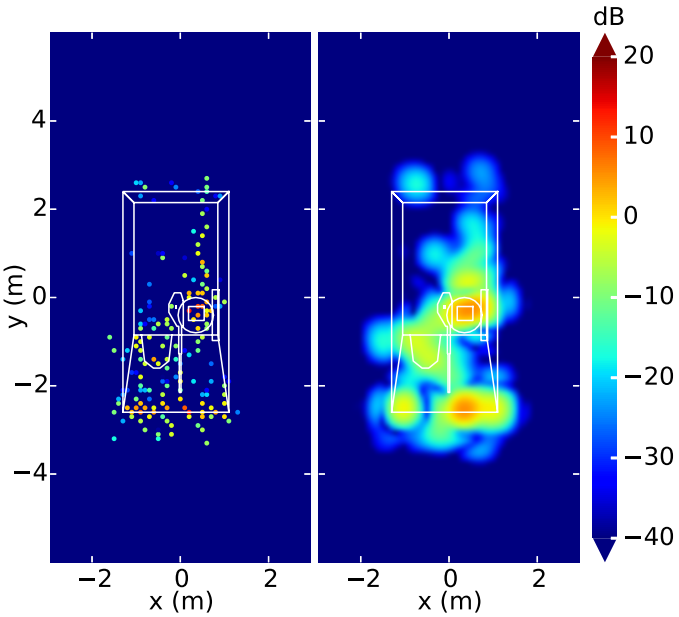

Fig. 7. Isotropic point reflector representation (left) and the corresponding back projection ISAR image (right) for the target with camouflage.

A synthetic point scatterer representation of the background is made as described previously. The clutter shown in the figures corresponds to a mean backscattering cross section per unit area or backscattering coefficient, σ_0, of -20 dB. This corresponds to a very low clutter level. [13] The noise level per unit are is set to -32 dB.

A target shadow is generated using a 3D CAD model of the target. Here an elevation angle of 10° is assumed for the SAR system. An outline overlay of the shadow on the point scatterers is shown in the left frame of Fig 8. The point scatterers inside the shadow region have been removed to simulate the effect of the shadow. The right frame shows the corresponding back projection ISAR images processed from the RCS generated by the forward operator, $\boldsymbol{A}$, operating on the matrix containing the point scatterer amplitudes.

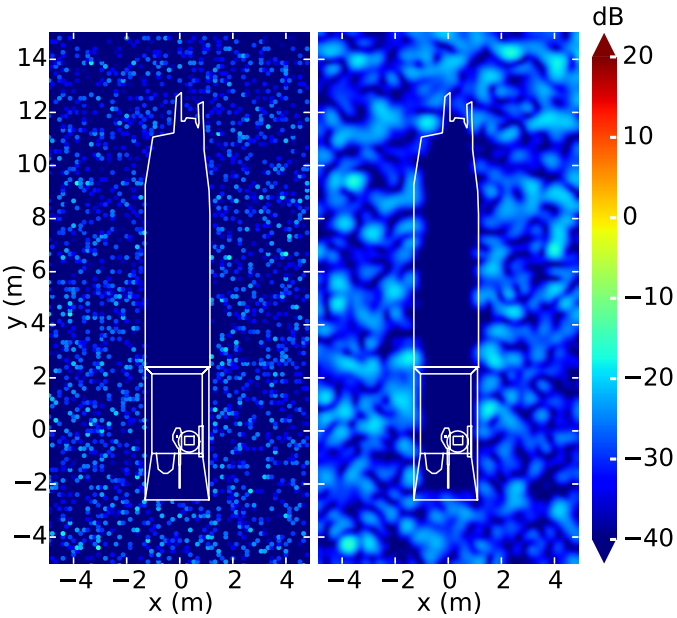

Fig. 8. Isotropic point reflector representation (left) and the corresponding back projection ISAR image (right) for the shadow of the target in the clutter background.

The shadow from the camouflage is generated in the same way also using a CAD model. An outline overlay of the shadow on the point scatterers is shown in the left frame of Fig 9. The background scatterers in the target shadow are removed as before while the scatterers in the shadow of the camouflage are attenuated corresponding to the nominal attenuation of the camouflage net. The corresponding back projection ISAR image shown in the right frame is then processed in the same way as described previously.

The point scatterers from the target measurement and the edited background are then merged together into new $\boldsymbol{z}$ matrices for both the target without camouflage and for the target with camouflage. Back projection images are then processed as described previously to generate RCS data. The results are shown in the left frames of Figs. 10 and 11 for the target without and with camouflage, respectively.

This procedure where ISAR images are blended into a SAR background results in seamless SAR images that can be used to evaluate *e.g.*, the efficiency of different camouflage with different detection algorithms.

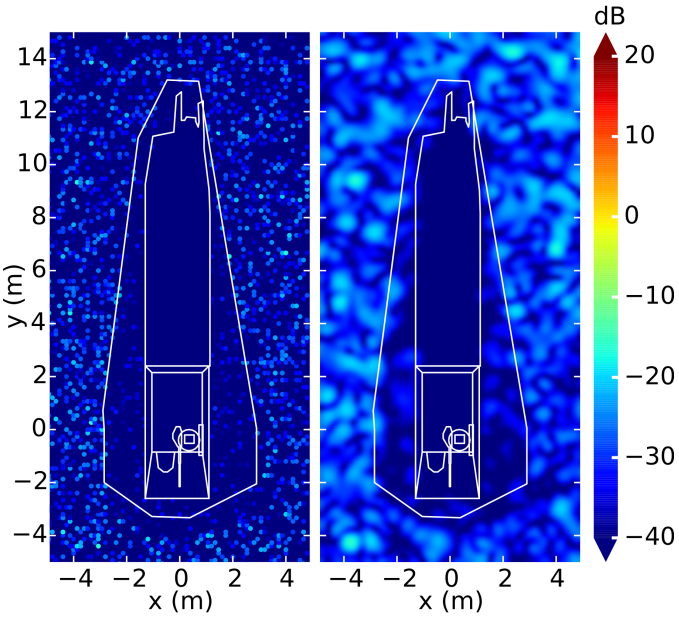

Fig. 9. Isotropic point reflector representation (left) and the corresponding back projection ISAR image (right) for the shadow of the camouflaged target in the clutter background.

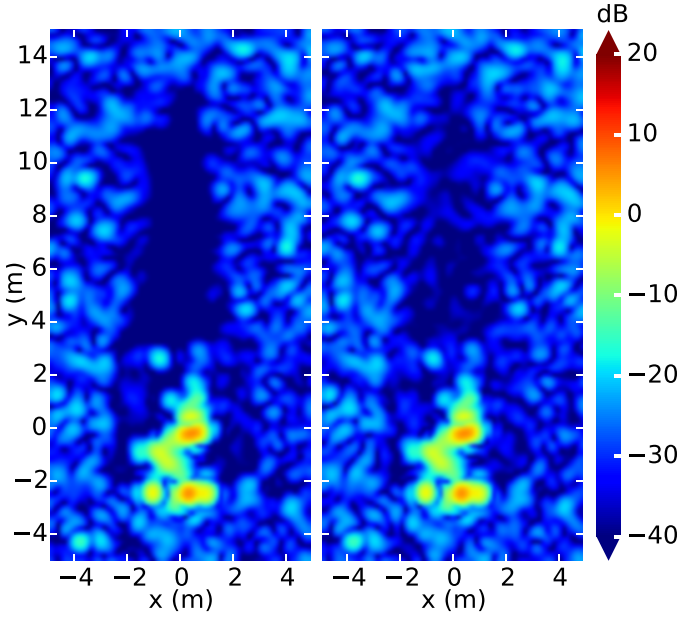

Fig. 11. Back projection ISAR image of the camouflaged target in a clutter background, without (left) and with (right) noise.

Noise is also added to the RCS to simulate the performance of a real SAR system. The right frames of Figs. 10 and 11 show the back projection images with added noise.

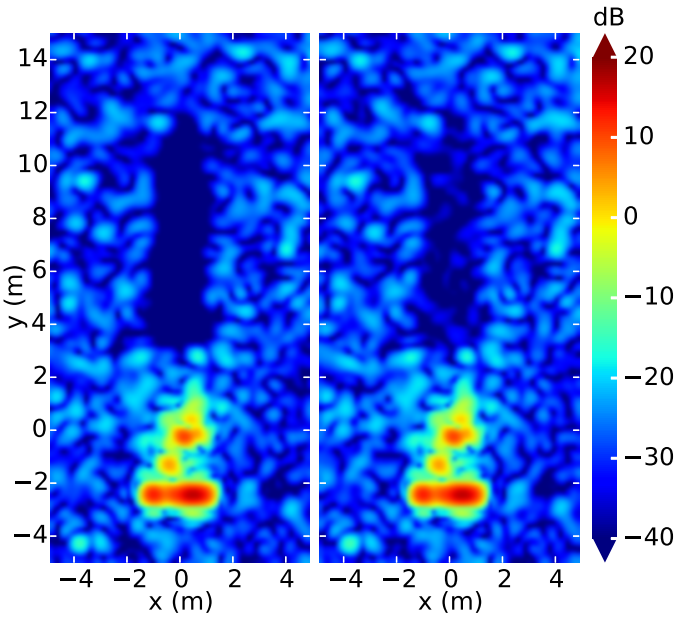

Fig. 10. Back projection ISAR image of the target in a clutter background, without (left) and with (right) noise.

V. Summary and Conclusions

We have shown how the compressed sensing method BPDN can be used to solve the inverse scattering problem for a model for a target with or without camouflage consisting of isotropic point scatterers. The target point scatterers are then merged into a SAR background that has been edited to show shadows from the target and the camouflage system.

The paper describes a method so that SAR images acquired in expensive airborne field trials can be used efficiently to evaluate different targets and camouflage measured separately in a ground based setup. The method is demonstrated with turntable measurements of a full scale target, with and without camouflage, signature extraction and blending into a SAR background. We find that the method provides an efficient way of evaluating measured target signatures in SAR backgrounds.

Acknowledgement

The financial support by the Swedish Defence Materiel Administration is gratefully acknowledged.

References

[1] T. D. Ross, S. W. Worrell, V. J. Velten, J. C. Mossing, and M. L. Bryant, "Standard SAR ATR evaluation experiments using the MSTAR public release data set," in *Aerospace/Defense Sensing and Controls*. International Society for Optics and Photonics, 1998, pp. 566–573.

[2] S. Bokaderov, M. Laubach, H. Schimpf, and P. Wellig, "EOSAR - A tool for the blending of real objects into SAR scenes," in *2011 German Microwave Conference (GeMIC)*. IEEE, 2011, pp. 1–4.

[3] E. J. Candès, J. K. Romberg, and T. Tao, "Stable signal recovery from incomplete and inaccurate measurements," *Communications on pure and applied mathematics*, vol. 59, no. 8, pp. 1207–1223, 2006.

[4] D. L. Donoho, "Compressed sensing," *IEEE Transactions on Information Theory*, vol. 52, no. 4, pp. 1289–1306, 2006.

[5] L. C. Potter, E. Ertin, J. T. Parker, and M. Cetin, "Sparsity and compressed sensing in radar imaging," *Proc. IEEE*, vol. 98, no. 6, pp. 1006–1020, 2010.

[6] E. van den Berg and M. P. Friedlander, "SPGL1: A solver for large-scale sparse reconstruction," June 2007, http://www.cs.ubc.ca/labs/scl/spgl1.

[7] ——, "Probing the pareto frontier for basis pursuit solutions," *SIAM Journal on Scientific Computing*, vol. 31, no. 2, pp. 890–912, 2008.

[8] V. M. Patel, G. R. Easley, D. M. Healy Jr, and R. Chellappa, "Compressed sensing for synthetic aperture radar imaging," in *2009 16th IEEE International Conference on Image Processing (ICIP)*. IEEE, 2009, pp. 2141–2144.

[9] B. Fischer, I. LaHaie, and M. Hawks, "On the use of basis pursuit and a forward operator dictionary to separate specific background types from target RCS data," in *Proc. Antenna Measurement Techniques Association (AMTA)*, Tucson, AZ, USA, 2014, pp. 85–90.

[10] T. Vaupel and T. F. Eibert, "Comparison and application of near-field ISAR imaging techniques for far-field radar cross section determination," *IEEE Trans. Antennas Propagat.*, vol. 54, no. 1, pp. 144–151, Jan. 2006.

[11] C. Larsson, "Nearfield RCS measurements of full scale targets using ISAR," in *Proc. Antenna Measurement Techniques Association (AMTA)*, Tucson, AZ, USA, 2014, pp. 1–6.

[12] J. Jersblad and C. Larsson, "Camouflage effectiveness of static nets in SAR images," in *Target and Background Signatures*, ser. Proc. SPIE, K. U. Stein and R. H. M. A. Schleijpen, Eds., vol. 9653, In press, 2015.

[13] F. T. Ulaby and M. C. Dobson, *Handbook of Radar Scattering Statistics for Terrain*. Norwood, MA, USA: Artech House, 1989.